ELSEVIER

Journal of Hazardous Materials 132 (2006) 98–110

Journal of Hazardous Materials

www.elsevier.com/locate/jhazmat

Assessment of environmental radon hazard using human respiratory tract models

K.N. Yu [a,*], B.M.F. Lau [a], D. Nikezic [b]

[a] *Department of Physics and Materials Science, City University of Hong Kong, Tat Chee Avenue, Kowloon Tong, Kowloon, Hong Kong, PR China*

[b] *Faculty of Sciences, University of Kragujevac, Serbia and Montenegro*

Available online 19 January 2006

Abstract

Radon is a natural radioactive gas derived from geological materials. It has been estimated that about half of the total effective dose received by human beings from all sources of ionizing radiation is attributed to ^{222}Rn and its short-lived progeny. In this paper, the use of human respiratory tract models to assess the health hazard from environmental radon is reviewed. A short history of dosimetric models for the human respiratory tract from the International Commission on Radiological Protection (ICRP) is first presented. The most important features of the newest model published by ICRP in 1994 (as ICRP Publication 66) are then described, including the morphometric model, physiological parameters, radiation biology, deposition of aerosols, clearance model and dose weighting. Comparison between different morphometric models and comparison between different deposition models are then given. Finally, the significance of various parameters in the lung model is discussed, including aerosol parameters, subject related parameters, target and cell related parameters, and parameters that define the absorption of radon from the lungs to blood. Dosimetric calculations gave a dose conversion coefficient of 15 mSv/WLM, which is higher than the value 5 mSv/WLM derived from epidemiological studies. ICRP stated that dosimetric models should only be used for comparison of doses in the human lungs resulted from different exposure conditions.

Keywords: Radon; Radon progeny; Human respiratory tract; Dose conversion coefficient; Lung cancer

1. Introduction

The main radioactive contaminant in the human environment is radon (^{222}Rn). It has been estimated that about half of the total effective dose received by human beings from all sources of ionizing radiation is attributed to ^{222}Rn and its short-lived progeny [1].

^{222}Rn is a natural radioactive gas and is a member of the natural radioactive series of ^{238}U. The seventh member of this series is ^{226}Ra with a half life of 1620 years. The earth crust, which mainly consists of soil and rocks, contains a certain amount of ^{226}Ra. The ^{226}Ra contents vary from one location to another, but is present almost everywhere. At some places it only appears as a trace element while at other places it is like an ore. By alpha decay of ^{226}Ra atoms, ^{222}Rn gas is formed. Being chemically inert, ^{222}Rn leaves the solid matrix in which ^{226}Ra atoms are confined and diffuses from the place of formation. Convective transport can also move ^{222}Rn atoms far from the place of origin. Radon migrates through the soil and may serve as an indicator of underground uranium ores. It can also pass the surface between the soil and the atmosphere and penetrate into the air. The readers are referred to the review by Fleischer [2] for a survey of radon transport processes.

Natural levels of ^{222}Rn in open space are usually below 10 Bq m^{-3}. This concentration does not present a significant radiation hazard. However, in closed space, like indoor environments, ^{222}Rn is accumulated due to poor ventilation. The ^{222}Rn concentration can reach a very high level if the source strength is large and the ventilation is poor. High radon concentrations in the order of a few hundreds of Bq m^{-3} or more can represent significant radiation hazards. On decay of ^{222}Rn, its short-lived progeny, ^{218}Po (α-particle emitter), ^{214}Pb (β-particle emitter), ^{214}Bi (β-particle emitter) and ^{214}Po (α-particle emitter) are formed. At the moment of creation in air, ^{218}Po is in the atomic stage, constituting the unattached (or free fraction of) radon progeny. Being chemically active, the progeny

* Corresponding author. Tel.: +852 27887812; fax: +852 27887830.
E-mail address: peter.yu@cityu.edu.hk (K.N. Yu).

0304-3894/$ – see front matter © 2005 Elsevier B.V. All rights reserved.
doi:10.1016/j.jhazmat.2005.11.087

tend to attach themselves to natural aerosols in the air to form the attached fraction. On inhalation, the attached or unattached radon progeny will enter the human lungs and will be deposited there. The emitted radiations damage the sensitive tissues in the lungs and may cause lung cancer. Some fractions of the radon progeny will also penetrate from the lungs into the blood and irradiate the whole human body. Furthermore, the long-lived radon progeny ^{210}Po is accumulated in the human bones.

Harmful effects of radon (and its progeny) are very well confirmed from underground uranium miners. There are several epidemiological studies that follow the health status of large populations of miners. These studies clearly show the relation between radon exposure and lung cancer incidences.

There are several special physical quantities and units in the field of radon science. The concentration of radon progeny is usually expressed through the quantity called potential alpha energy concentration (PAEC) defined as total energy of alpha particles emitted by the radon progeny in a unit volume of air. It is calculated from the formula

$$\mathrm{PAEC} = \sum_{i=1}^{4} C_i E_i \tag{1}$$

where C_i is the number of atoms of the ith radon progeny in $1\,\mathrm{m}^3$ of air and E_i is the corresponding potential alpha energy in Joule (J). The SI unit for the PAEC is $\mathrm{J\,m^{-3}}$; while the traditional and the still very commonly used unit working level ($\mathrm{WL} = 2.08 \times 10^{-5}\,\mathrm{J\,m^{-3}}$). The exposure to radon progeny X is the product of the average PAEC and the exposure time t of the exposure:

$$X = \mathrm{PAEC} \times t \tag{2}$$

and expressed in $\mathrm{J\,s\,m^{-3}}$. The traditional unit in use is called the working level month (WLM).

The exposure of the human body to ionizing radiation, including radiation from radon and progeny, is characterized by the effective dose E, which is a weighted absorbed dose [3]. There are two kinds of weighting, namely, according to the type of radiation and according to the type of irradiated tissue. The effective dose is defined as

$$E = \sum_{T} w_T \sum_{R} w_R D_R \tag{3}$$

where D_R is the *mean* absorbed dose in the organs or tissues irradiated by the radiation R, w_R the radiation weighting factor that accounts for the differences among various types of radiation and w_T is the tissue weighting factor which takes into account the different sensitivities of various tissues in the human body to radiations. The tissue weighting factor for the human lung is $w_L = 0.12$. The SI unit for the effective dose is Sievert (Sv). The effective dose is not a measurable quantity and is a subject of calculations only. To calculate the effective dose, some models, called dosimetric models, are needed. In other words, a dosimetric model of the human respiratory tract is needed for dose calculations in the human lung.

Determination of the effective dose in the human lung for a given exposure condition is a very complicated task. To enable the calculations, one should determine the absorbed dose in the sensitive cells and perform weightings for them. The result is the so-called dose conversion coefficient (DCC) which represents the effective dose per unit exposure to radon progeny, and the common unit for DCC is mSv/WLM.

In addition, some other tasks of dosimetric modeling are performed, such as

- To make possible prediction, dose estimation and to be useful for limit derivation.
- To take into account the influence of smoking and other air pollutants as well as respiratory tract diseases.
- To enable calculations for other lung pollutants like gases and vapors, etc.

2. History of ICRP dosimetric models for the human respiratory tract

In this section, a short history of dosimetric models for the human respiratory tract is presented. The International Commission on Radiological Protection (ICRP) is the international body that collects and critically considers all relevant data on ionizing radiation and its effects on human, and issues recommendation in the form of publications. Until now, about 90 ICRP publications have been issued. In addition, there are other international or national commissions concerning the ionizing radiation, e.g., the International Commission on Radiological Units (ICRU), Biological Effects of Ionizing Radiation (BEIR) Committee, National Council of Radiation Protection (NCRP), etc. The human respiratory tract models have been mainly dealt with by ICRP although other commissions are also involved.

Dosimetric modeling of the respiratory tract started soon after the Second World War in 1949 in relation to the enhanced necessity for nuclear technology and uranium ore exploring. The needs for standardization of values for parameters describing inhalation, deposition, retention and translocation of airborne radionuclides in workers for the purpose of deriving exposure limits were recognized. The first conference devoted to dosimetric models of the human respiratory tract was held in 1949 at Chalk River, Canada. Different aspects of aerosol particle deposition and retention were discussed, and the large deficiency of information was noted. It was agreed that 50% of any inhaled aerosols reached the alveoli and that soluble particles would be completely absorbed. If the aerosol particles were insoluble, half of them would be retained for 24 h, and half of the remaining (25% of inhaled quantity) would be retained indefinitely. In the following meetings, different parameters which could influence the deposition and retention of inhaled aerosols were identified. These parameters included the particle size and shape, surface area available for deposition, and breathing habits (nose or mouth breathing), etc.

This very simple model of the deposition was slightly improved in 1953 at the "Arden House Conference" when it was assumed that 50% of inhaled aerosols were deposited in the upper part of the respiratory tract, 25% would be exhaled and 25% would be retained in the lungs. If the particles were soluble, 25% would be absorbed and translocated to different organs

in the body. For insoluble particles, 12.5% would be cleared in 24 h, and the remaining 12.5% would be retained with a half time of 120 d. This model of deposition, retention and clearance of inhaled aerosol particles was the basis for the limits for exposure to radionuclides in ICRP Publication 2 [4] as well as for the calculation of doses to exposed individuals.

In 1964, the ICRP Committee 2 appointed a Task Group on Lung Dynamics to review the previous model published in the ICRP Publication 2. Two years later, a new lung model was published [5] with a greatly improved lung deposition and clearance models. Many innovations were introduced by the Task Group. Three different regions of the respiratory tract were recognized (nosopharyngeal, tracheobronchial tree and pulmonary), and the term "anatomical compartments" were introduced. The deposition models in different compartments were based on dust sampling data. This 1966 model also considered particle size and breathing rate with respect to the fraction deposited in different region of the lungs.

The second important feature was the quantitative kinetic clearance model that described the removal of materials deposited in each of the three regions. The new concept was the classification of chemical compounds according to their tendency to be dissolved in the respiratory tract fluids, which was known as the DWY classification. Class D referred to highly soluble compounds that were cleared from the respiratory tract with clearance half time less than 1 d. Class W referred to less soluble compounds that were cleared from the respiratory tract with clearance half time of a few days to months. Finally, Class Y referred to more insoluble compounds that were expected to be retained in the respiratory tract with half time of 6 months to 1 year.

However, this greatly improved model was not formally accepted for dose limit calculations until 1979 when the new ICRP 30 Publication [6] was prepared. In this publication, the derived air concentration and the annual limits on intake were introduced. Furthermore, the transfer of radioactive materials to the lymph nodes was included in this model. These models calculated the dose in the total mass of the blood filling lungs, and they did not recognize specific sensitive cells in the epithelium. Filtration in nasal passage was also not considered in this model.

Since 1966, many extensive investigations in the field had been undertaken, and many deficiencies of the model were observed. The most important criticism was addressed to the DWY classification of chemical compounds. Many materials were cleared from the human respiratory tract at rates considerably different from the predicted ones. On the other hand, some materials did not fit any of the categories in the classification. A very important case was found for inhalation of the highly insoluble plutonium oxide which was cleared with a rate smaller than that for the Y class.

In addition, investigations had extended to particles with diameters smaller than those considered in the 1966 model. The model presented in the ICRP 30 is related to the occupational exposure of reference Caucasian males. However, in the last two decades, interest had been raised about public exposure to radioactivity in the environment. A new model was therefore necessary to enable dose calculations for other members of the population as well as for other ethnical groups in the world.

Radiobiological investigations had shown large differences in radio-sensitivity of different cells in the respiratory tract. In ICRP 32 [1], the dose was calculated in basal cells in the bronchial epithelium and in the pulmonary region. Half of the stochastic risk was associated with these regions, which was contradictory to the previous concept of mean lung dose used in ICRP 30. Further radiobiological studies had included secretory cells as target cells at risk.

All these new findings and deficiencies of old models had requested for a new respiratory tract model. As a result, the ICRP formed a new Task Group on Lung Dynamics in 1984 in order to review the old model and to propose modifications and improvements of the existing respiratory tract model. The new model appeared in 1994 (the ICRP66 model) in ICRP Publication 66 [7]. This rather comprehensive report was a collection of almost all knowledge in this field at that time. In the following, the most important features of this model will be described.

Softwares that implemented the ICRP66 model were available, namely, the LUDEP program [8] and its smaller version RADEP for radon [9]. In addition to these, there were several home written programs that follow ICRP66 recommendations. These softwares enabled calculations of DCCs and analyses of influence of different relevant parameters on the lung dose.

3. ICRP66 dosimetric models for the human respiratory tract

The ICRP66 model (published in 1994) consists of six submodels, for the:

(a) morphometry, which describes the structure of the respiratory tract and the important dimensions;
(b) respiratory physiology, which determines the rate and volume of inhaled air;
(c) radiation biology, which determines the sensitive cells that are at risk and where lung cancer develops;
(d) deposition of radioactive aerosols in different regions of respiratory tract;
(e) clearance of the deposited materials, including different pathways and translocations of the materials;
(f) dosimetry, which calculates the dose in the target tissues, and includes dose weighting.

In the following discussions, each of these sub-models will be described in some more details.

3.1. Morphometric model

ICRP described the morphological characteristics of the respiratory tract, defined the morphometric model for dose calculations and gave the nominal values for the parameters used in the dosimetric model. The respiratory tract consists of four anatomical regions:

(1) the extrathoracic region, ET, which consists of the anterior nose (ET_1) and the posterior nasal passages, larynx, pharynx and mouth (ET_2);
(2) the bronchial (BB) region consisting of the trachea and bronchi, i.e., from generation 0 (trachea) up to generation 8;
(3) the bronchiolar (bb) region consisting of bronchioles and terminal bronchioles, i.e., from generation 9 to generation 15;
(4) the alveolar interstitial (AI) region consisting of respiratory bronchioles, alveolar ducts and sucs with their alveoli, and interstitial connective tissue.

Lymphatic tissues, nodes, capillaries and vessels are present in all regions of the respiratory tract. The lymphatic nodes LN_{ET} are in the extrathoracic region and they collect fluids from this region. The nodes LN_{TH} are located in the BB region but collect fluids from all thoracic parts of the respiratory tract.

The real structure of the respiratory tract is rather complicated, but for the purposes of dose calculations some simplified geometries are adopted. The typical airway is represented as a cylindrical tube of an internal caliber and wall thickness, which is shown in Fig. 1.

The wall of the airway tube consists of a few layers. The radioactive source is in the mucus layer where the radioactive aerosols are mixed with the mucus gel. Since alpha particles emitted by short-lived radon progeny have short ranges in tissues, the thickness of the layers represented in Fig. 1 are of significant importance for dose calculations.

3.1.1. Extrathoracic region (ET)

The air is inspired through the nose (except when the nose is blocked or during heavy physical exercises). The main task of this region is to clean the inspired air and to conduct it to the lung. This part will also warm and damp the inhaled air. The temperature and humidity in the ambient air are usually lower than those in the lung. Cleaning is achieved by impactional and/or diffusion deposition in the narrow nasal passages which have a slit shape formed by convoluted turbinates. The airflow changes direction a few times in this part, which enhances the impactional deposition.

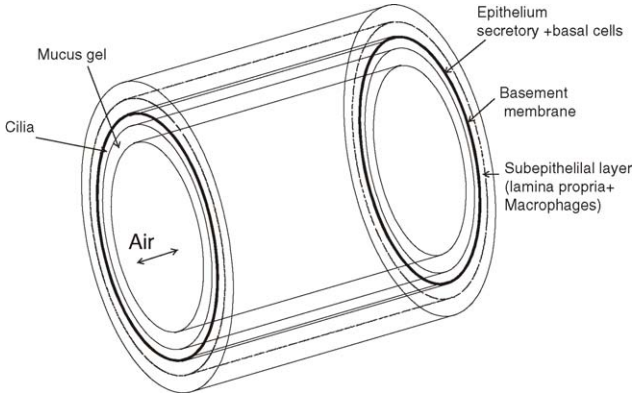

Fig. 1. A simplified geometry of the airway tube (adopted from Ref. [7]).

After the nasal passage, the inspired air enters into the pharynx and continues vertically down through the oral part of the pharynx into the larynx and the trachea. The larynx contains the vocal cord and the space between them is of a slit shape so that deposition of aerosol particles is enhanced in this region.

In the ET_1 region, the walls are covered with skin where radioactive aerosols can deposit. The dimensions of this part are as follows:

(a) average thickness of the skin: 50 μm;
(b) average depth of the nuclei of sensitive basal cells: 40–50 μm;
(c) total surface area: 20 cm^2;
(d) equivalent average diameter of air passage: 5 mm.

The walls in the ET_2 region are covered partially with ciliated, pseudostratified epithelium, and partially by stratified squamous epithelium. The dimensions in the ET_2 region are summarized as

(a) equivalent average diameter of air passage: 3 cm;
(b) average thickness of mucus layer: 15 μm;
(c) average thickness of stratified squamous epithelium: 50 μm;
(d) average depth of the nuclei of sensitive basal cells: 40–50 μm;
(e) total surface area: 450 cm^2.

3.1.2. Bronchial (BB) region

This region is the most interesting one for radiation protection considerations because the majority of lung cancer originates in this part of the respiratory tract. The BB region includes the trachea (generation 0), main bronchi (generation 1) and other bronchi up to generation 8, as well as lymph vessels and nodes. This region, together with the bronchiolar (bb) region, looks like a tree, and is sometimes called the tracheo-bronchial tree (or T-B tree in short).

The trachea is divided into two main bronchi, which divide into the lobar bronchi, three on the right hand side and two on the left hand side. The lobar bronchi divide further into segmental bronchi. Although the human lungs are not completely symmetrical, the ICRP adopted that the bronchi divide dichotomously (so the ICRP66 model neglected irregularities in branching and the asymmetry of the human lungs). The number of airway tubes for the nth generation is then equal to 2^n. If asymmetry is taken into account, the number of tubes will not be exactly equal to 2^n. This assumption may have an influence on the total surface area available for deposition; this is an important parameter because a larger surface area means a smaller activity per unit surface (for the same deposited activity) and consequently a lower dose.

The dimensions and geometry of the T-B tree are very important in deposition and other calculations. There are relatively few experimental data on the dimensions (diameters and lengths) of airway tubes, and with rather large discrepancies among different authors. In the ICRP66 model, the dimensions from three sources, Weibel [10], Yeh and Schum [11] and Phalen et al. [12] were averaged and adjusted to the standard functional residual capacity (FRC). These average and adjusted dimensions are given in Table 1.

Table 1
Diameters and lengths of airways in the BB and bb regions according to the ICRP66 model (adopted from Ref. [7])

Generation	Diameter (cm)	Length (cm)
0 (trachea) BB	1.65	9.1
1 (main bronchi)	1.2	3.8
2	0.85	1.5
3	0.61	0.83
4	0.44	0.9
5	0.36	0.81
6	0.29	0.66
7	0.24	0.60
8	0.2	0.53
9 (bb)	0.1651	0.4367
10	0.1348	0.362
11	0.1092	0.3009
12	0.0882	0.25
13	0.072	0.2069
14	0.0603	0.17
15 (terminal bronchioles)	0.0533	0.138

The structure and thickness of the bronchial wall are important in dose calculations. The model for the typical bronchial wall is shown in Fig. 2. The sensitive cells are secretory and basal cells, whose territories partially overlap and both are in the epithelium tissue. The doses in the tracheal epithelium need not be calculated because the epithelial tissue is too thick and alpha particles cannot reach the sensitive cells.

The following morphological dimensions for the BB region are recommended for dose calculations:

(a) volume of trachea and bronchi: 5×10^{-5} m^3;
(b) surface area (generations 1–8): 2.9×10^{-2} m^2;
(c) average caliber: 5 mm;
(d) the thickness of the layers: as shown in Fig. 2.

3.1.3. Bronchiolar (bb) region

This region consists of airway tubes between generations 9 and 15. The last generation (15) is called terminal bronchioles. Their dimensions are also given in Table 1. All airways in generations $n > 15$ carry alveoli. The basal cells are rarely present in this region, and the target cells in the bb region are the secretory cells (the special type called Clara cells).

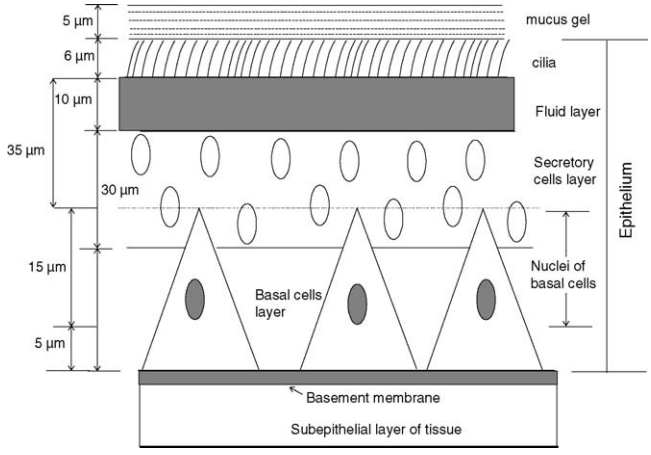

Fig. 2. Model of the bronchial wall in the BB region (adopted from Ref. [7]).

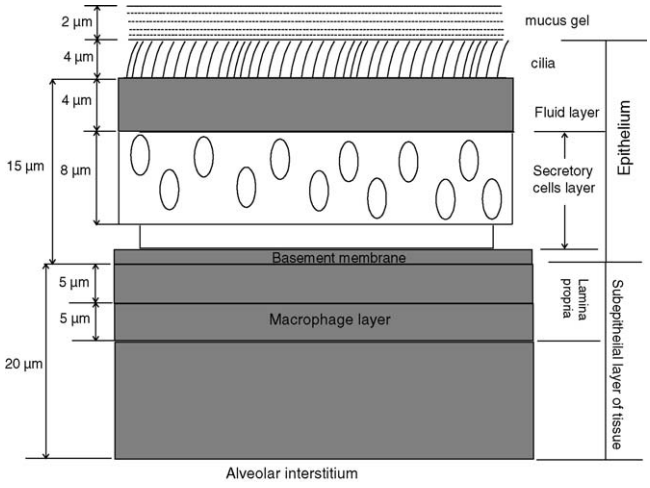

Fig. 3. Model of the bronchiolar wall in the bb region (adopted from Ref. [7]).

The model of the wall of the bronchioles is given in Fig. 3. The following morphological dimensions for the bb region are recommended for dose calculations:

(a) volume of bronchioles (generations 9–15): 5×10^{-5} m^3;
(b) surface area (generations 9–15): 2.4×10^{-1} m^2;
(c) thickness of the layers: as shown in Fig. 3;
(d) average caliber: 1 mm.

3.1.4. Alveolar interstitial region (AI)

This region starts from the terminal bronchioles and includes generations 16–26, i.e., the respiratory bronchioles and the alveolar ducts, as well as lymph vessels, nodes and lymphatic tissue. The dimensions for this region are given in Table 2. The main task of this region is gas exchange. The total volume of the respiratory bronchioles is 2×10^{-4} m^3 and the total surface area is 7.5 m^2. The volume of alveoli ducts and sacs is approximately 4.5×10^{-3} m^3 while the surface area is very large and is about 140 m^2.

Table 2
Morphological model of the bb region (adopted from Ref. [7])

Generation	Diameter (m)	Length (m)
1 (respiratory bronchioles)	5.1×10^{-4}	1.1×10^{-3}
2 (respiratory bronchioles)	4.6×10^{-4}	9.2×10^{-4}
3 (respiratory bronchioles)	4.1×10^{-4}	7.6×10^{-4}
4 (alveolar ducts)	3.8×10^{-4}	6.3×10^{-4}
5 (alveolar ducts)	3.5×10^{-4}	5.2×10^{-4}
6 (alveolar ducts)	3.3×10^{-4}	4.3×10^{-4}
7 (alveolar ducts)	3.1×10^{-4}	3.6×10^{-4}
8 (alveolar ducts)	3.0×10^{-4}	3.0×10^{-4}
9 (alveolar ducts)	2.9×10^{-4}	2.1×10^{-4}
10 (alveolar ducts)	2.8×10^{-4}	2.1×10^{-4}
11 (alveolar ducts)	2.8×10^{-4}	1.7×10^{-4}

Table 3
Reference values for Caucasian workers (30 years old, 176 cm height, and 73 kg weight) (adopted from Ref. [7])

Lung volumes		Values (l)
Total lung capacity (TLC)		6.98
Functional residual capacity (FRC)		3.30
Vital capacity (VC)		5.02
Dead space (V_d)		0.146
Ventilation rates	V_E (l/min)	B ($m^3\ h^{-1}$)
Sleep	7.5	0.45
Rest, sitting	9.0	0.54
Light exercise	25	1.5
Heavy exercise	50	3.0

3.2. Physiological parameters

The physiological parameters relevant for the dosimetric model are: the total lung capacity TLC, functional residual capacity FRC, vital capacity VC, dead space V_d, tidal volume V_T (all in liters), ventilation rates V_E (in l/min), breathing rate B (in $m^3\ h^{-1}$) and breathing frequency f_R (breath per min).

The radiation doses in the respiratory tract are controlled to a great extent by the breathing characteristics and habits. These determine the activity of the inhaled radioactive particles and their penetration and deposition in the respiratory tract. Since the breathing parameters vary significantly among the world population, a respiratory tract model that could be applied to all ethnical groups is neither feasible nor necessary. Reference values for Caucasian workers have been given in the ICRP66 report. A second set of parameters is given for Caucasian male and female non-workers of all ages. Direction has also been given to adapt these values for other ethnic groups. The reference respiratory values for workers are given in Table 3.

The reference values for other members (i.e., non-workers) of the Caucasian population have been given in the ICRP66 report, including those for children of 3 months, 1, 5, 10 and 15 years old, and those for adults (both male and female). Examples of variation of respiratory tract parameters for different ethnic groups in the world population (Japan, China, India, US-black, Senegal and Zimbabwe) have also been given in the ICRP66 report.

3.3. Radiation biology

The ICRP66 dosimetric model is based on the assumption of different sensitivities of various tissues and cells in the human respiratory tract to ionizing radiation, so that calculations of doses in different regions are necessary. All regions of the human respiratory tract are sensitive to radiation, but with different sensitivities. The cells and tissues at risk are identified and their relative radio-sensitivities are attributed through radiobiology. The report recommended factors for weighting the doses in different tissues, so that one value for the thoracic region and one value for the extrathoracic region can be obtained.

In Chapter 4 of the ICRP66 report, relevant data about cancer incidences and their locations in the human respiratory tract are given. The types of cancers appearing in the extrathoracic and thoracic regions are considered separately. In the thoracic region, there are four main classes of cancers, i.e., (1) squamous cell carcinoma, (2) small cell carcinoma, (3) adenocarcinoma, and (4) large cell carcinoma. It is not possible to determinate the locations of cancer origin; only the region of cancer (ET, BB, bb or AI) in the ICRP scheme can be determined.

The cells of origin of these cancers are not unequivocally known. It was concluded, after radiobiological consideration, that basal cells and secretory cells were most probably the progenitors for cancer development and that they should be included in dose calculations. Lymph tissue and lymph nodes were considered as insensitive to radiation.

In a population that is exposed only to natural radiation, about 3/4 of the squamous cancers and small cell cancers, 1/4 of the adenocarcinoma and 1/2 of the large cell carcinoma have originated in the BB region (in generations 1–8). The rest of the squamous cell cancers, small cell cancers, large cell cancers and 1/2 of adenocarcinoma have originated in the bb region (generations 9–15). The rest of adenocarcinoma is in the AI region. Therefore, squamous and small cell carcinomas originate in the central part while adenocarcinoma is the illness of the peripheral part of the T-B tree. Large cell cancers appear in both the central and the peripheral part, but with different frequency (3/4 in central part).

These data indicate that uniform irradiation of the human lung produces cancers in the BB region with the largest probability. However, the existing set of experimental data is not enough for quantification of relative sensitivity of the BB, bb, and AI regions. Therefore, the ICRP proposed equal risks for these three regions of the human lung. The equivalent doses should then be calculated according to the following equations:

$$H_{ET} = H_{ET_1} A_{ET_1} + H_{ET_2} A_{ET_2} + H_{LNET} + H_{LNET} \quad (4)$$

$$H_{TH} = H_{BB} A_{BB} + H_{bb} A_{bb} + H_{AI} A_{AI} + H_{LNTH} A_{LNTH} \quad (5)$$

where H_{ET} and H_{TH} are equivalent doses in the extrathoracic and thoracic regions, respectively, which are weighted according to the radiation detriment of the particular region, H_i are the equivalent doses in the ith region, and A_i are factors for apportionment of radiation detriment for the ith region, as given in Table 4.

Table 4
Weighting factors assigned for the partition of radiation detriment among different respiratory tract regions (adopted from Ref. [7])

Tissue	A
Extrathoracic region	
ET_1 (anterior nose)	0.001
ET_2 (posterior nose, larynx, pharynx, mouth)	1
LN_{ET}	0.001
Thoracic region	
BB (bronchial, generations 1–8)	0.333
bb (bronchiolar, generations 9–15)	0.333
AI (alveolar-interstitial)	0.333
LN_{TH}	0.001

The final step is calculation of the effective dose (previously known as effective dose equivalent) as the measure for the total radiation detriment. The ICRP recommended the value 0.12 for the tissue weighting factor w_T for the human lung. Other tissues of the respiratory tract were not listed in their report.

3.4. Deposition of aerosols in human respiratory tract

Deposition of inhaled aerosols is one of the most important issues in the human respiratory tract model. This problem has been extensively studied in the past and a comprehensive literature survey is given in Annex D of the ICRP66 report. The deposition model is needed to provide the fraction of inhaled aerosols to be deposited in the human lung. The model described the deposition of aerosols in a very wide range of diameters, from atomic dimensions up to about 0.1 mm. It is also applicable to different individuals under various exposure conditions, and enables calculations of deposition for gases and vapors.

The aerosols are mixed in air and they enter into the human lung during inhalation. A fraction of them is deposited in the lung while the rest is ejected from the body during exhalation.

There are two groups of deposition processes, i.e., thermodynamic and aerodynamic deposition. The former is characteristic for small-diameter particles and is often called diffusion or Brownian deposition. This type of deposition is caused by the random movement of the aerosols in the air stream. When the aerosols "touch" the wall of the airway tube, they can stay in that position. Aerodynamic deposition is more important for larger particles and there are two types of processes belonging to this group. The first one is "impactional" or inertial deposition. This deposition process takes place when the air stream changes the direction; some of the airborne aerosols with larger mass cannot adjust their directions of movement sufficiently quickly because of their inertia, and impact onto the wall of the airway tube. The second aerodynamic deposition process is gravitational sedimentation of aerosols. There are also other less important deposition processes like interception, which is important for fibers, etc.

Deposition occurs in all compartments of the human lung, but with different efficiencies. The deposition pattern depends on the aerosol diameter as well as airflow characteristics.

The behavior of small-size particles (which are deposited by diffusion) is described in terms of the thermodynamic diameter d_{th} and the diffusion coefficient D. Deposition of larger particles is described by the aerodynamic diameter d_{ae}. The aerodynamic diameter is defined in terms of the equivalent particle volume diameter d_e (i.e., the diameter of a spherical particle with the same volume as the considered particle) by the following formula:

$$d_{ae} = d_e \sqrt{\frac{\rho C(d_e)}{\chi \rho_0 C(d_{ae})}} \tag{6}$$

where ρ is the particle density, $\rho_0 = 1\,\mathrm{g\,cm^{-3}}$ (unit density), χ the particle shape factor (its value is usually between 1 and 2), and C is the so-called Cunningham correction slip factor given as

$$C(d) = 1 + \frac{\lambda}{d_e}[2.514 + 0.8\,\mathrm{e}^{-0.55(d_e/\lambda)}] \tag{7}$$

where $\lambda = 0.0712\,\mu\mathrm{m}$ is the mean free path of air molecules at 37 °C, 100% relative humidity and 760 mmHg atmospheric pressure. The parameter d_{ae} appears on both sides of Eq. (6) and iterations should be used in order to determine d_{ae}.

The thermodynamic diameter is given in terms of its aerodynamic diameter by the following equation:

$$d_{th} = d_e \sqrt{\frac{\chi \rho_0}{\rho} \frac{C(d_{ae})}{C(d_{th})}} \tag{8}$$

This equation, again, needs to be solved by iterations in order to find d_{th}.

If both kinds of deposition processes (thermodynamic and aerodynamic) are present, the combined effect is given as a quadratic sum:

$$\eta = \sqrt{\eta_{th}^2 + \eta_{ae}^2} \tag{9}$$

where η is the total deposited fraction, while η_{th} and η_{ae} are the thermodynamic and aerodynamic deposition fractions.

For particles with thermodynamic diameters smaller than 0.1 μm, diffusion deposition is dominant. If the aerodynamic diameter is larger than 1 μm, aerodynamic deposition is the most important.

3.4.1. The recommended ICRP66 deposition model

The ICRP66 deposition model estimates regional deposition, i.e., deposition in each anatomical region of the respiratory tract. A semi-empirical approach has been used to describe the regional deposition. Relative simple algebraic equations derived from experiments and theory are used for the deposition model.

Each breath is represented by a tidal flow of air that carries particles through each anatomical region which is represented by one or more filters in series. A filter j has two parameters, i.e., the volume v_j and the filtration efficiency η_j, and Φ_j is the fraction of the tidal volume (denoted by V_t) which passes through the filter j. During inhalation, smaller and smaller fractions of the tidal volume pass through the filters in turn, which are determined by the cumulative volumes of the preceding filters. During exhalation, the same volume of air passes through the same filters as those during the inhalation. The filtration efficiency η_j of the filter j is the fraction of particles incident on the filter which is deposited.

The filtration efficiency (which is equal to the deposition efficiency) for an anatomical region is given in the form

$$\eta = 1 - \mathrm{e}^{-aR^p} \tag{10}$$

where a and p are parameters and R is a function of the particle diameter and flow rate. The function in Eq. (10) is given separately for thermodynamic and aerodynamic depositions.

The ICRP66 model is also able to take into account the breathing habit since depositions in the nose and the mouth are different. Table 5 gives recommended parameters and functions for the regional aerodynamic deposition, and Table 6 gives

Table 5
Recommended algebraic expressions for aerodynamic deposition (adopted from Ref. [7])

Phase	Filter	Region	Aerodynamic regional deposition $\eta_{ae} = 1 - \exp(-aR^p)$		
			a	R	p
Inspiration	1	ET_1	3×10^{-4}	$d_{ae}^2 V_n \, SF_t^3$	1
	2	ET_2	5.5×10^{-5}	$d_{ae}^2 V_n \, SF_t^3$	1.17
	3	BB	4.08×10^{-6}	$d_{ae}^2 V_n \, SF_t^{2.3}$	1.152
	4	bb	0.1147	$(0.056 + t_b^{1.5}) \times d_{ae}^t t_b^{-0.25}$	1.173
	5	AI	$0.146 \times SF_A^{0.98}$	$d_{ae}^2 t_A$	0.6495
Expiration	6	bb	0.1147	$(0.056 + t_b^{1.5}) \times d_{ae}^t t_b^{-0.25}$	1.173
	7	BB	2.04×10^{-6}	$d_{ae}^2 V_n \, SF_t^{2.3}$	0.152
	8	ET_2	5.5×10^{-5}	$d_{ae}^2 V_n \, SF_t^3$	1.17
	9	ET_1	3×10^{-4}	$d_{ae}^2 V_n \, SF_t^3$	1

the corresponding information for thermodynamic deposition, both for the fraction inhaled through the nose. Here ψ_{th} is the empirical correction factor to allow for enhancement of thermodynamic deposition caused by turbulent airflow in the first few generations of the T-B tree; and

$$V'_D(BB) = V_D(BB)\left(1 + \frac{V_T}{FRC}\right) \tag{11}$$

and

$$V'_D(bb) = V_D(bb)\left(1 + \frac{V_T}{FRC}\right) \tag{12}$$

t is the residence time of air in an anatomical region, and SF are scaling factors from a Caucasian adult male to some other subjects. A scaling factor is defined as the ratio of a reference airway size in an adult Caucasian male to that in the subject. The characteristic airway size in the ET and BB regions is taken to be the diameter of the trachea. For the bb and AI regions, the characteristic airway sizes are the diameters of airways in the 9th and 16th generations, respectively.

For mouth breathing, there is no deposition in the ET_1 region. The deposition in ET_2 is different in this case and the parameters are given in Table 7. The functions and parameters for the deposition in other regions are the same as those in the case of nose breathing.

The residence times are given by the following equations:

$$t_B = \frac{V_D(BB)}{V}\left(1 + \frac{0.55V_T}{FRC}\right) \tag{13}$$

$$t_b = \frac{V_D(bb)}{V}\left(1 + \frac{0.55V_T}{FRC}\right) \tag{14}$$

$$t_A = \frac{V_T - V_D(ET) - [V_D(BB) + V_D(bb)]\left(1 + \frac{V_T}{FRC}\right)}{V} \tag{15}$$

3.4.2. Deposition of polydispersed aerosols

Aerosols consist of particles with different size, which are usually distributed according to the log-normal distribution. The parameters characterizing the deposition of activity in the respiratory tract are the activity median aerodynamic diameter (AMAD) for aerodynamic deposition, and the activity median thermodynamic diameter (AMTD) for thermodynamic deposition.

The total deposition of polydispersed aerosols in an anatomical region is obtained as a weighted sum of the deposition of monodispersed aerosols. The weighting is carried out according to the fraction of aerosols within the specific diameter range.

3.4.3. Application of the deposition model

ICRP recommended a set of values for the different variables in the deposition model described above. The following default values were recommended:

Table 6
Recommended algebraic expressions for thermodynamic deposition (adopted from Ref. [7])

Phase	Filter	Region	Thermodynamic regional deposition ($\eta_{ae} = 1 - \exp(-aR^p)$)			Volumetric fraction
			a	R	p	
Inspiration	1	ET_1	18	$D(V \times SF_t)^{-1/4}$	1/2	1
	2	ET_2	15.1	$D(V \times SF_t)^{-1/4}$	0.538	1
	3	BB	$22.02 \times SF_t^{1.24}\psi_{th}$	Dt_B	0.6391	$1 - V_D(ET)/V_t$
	4	bb	$-76.8 + 167 \times SF_b^{0.65}$	Dt_b	0.5676	$1 - [V_D(ET) + V'_D(BB)]/V_T$
	5	AI	$170 + 103 \times SF_A^{2.13}$	Dt_A	0.6101	$1 - [V_D(ET) + V'_D(BB) + V'_D(bb)]/V_T$
Expiration	6	bb	$-76.8 + 167 \times SF_b^{0.65}$	Dt_b	0.5676	$1 - [V_D(ET) + V'_D(BB)]/V_T$
	7	BB	$22.02 \times SF_t^{1.24}\psi_{th}$	Dt_B	0.6391	$1 - V_D(ET)/V_t$
	8	ET_2	15.1	$D(V \times SF_t)^{-1/4}$	0.538	1
	9	ET_1	18	$D(V \times SF_t)^{-1/4}$	1/2	1

Table 7
Deposition for mouth breathing (adopted from Ref. [7])

Phase	Filter	Region	Aerodynamic deposition ($\eta_{ae} = 1 - \exp(-aR^p)$)			Thermodynamic deposition ($\eta_{th} = 1 - \exp(-aR^p)$)		
			a	R	p	a	R	p
Inspiration	1	ET_2	1.1×10^{-4}	$d_{ae}^2(V \times SF_t^3)^{0.6} \times (V_T \times SF_t^2)^{-0.2}$	1.4	9	$D(VF_t)^{-1/4}$	1/2
Expiration	7	ET_2	1.1×10^{-4}	$d_{ae}^2(V \times SF_t^3)^{0.6} \times (V_T \times SF_t^2)^{-0.2}$	1.4	9	$D(VF_t)^{-1/4}$	1/2

(a) AMAD = 1.5 μm for workplace exposure;
(b) AMAD = 1 μm for indoor and outdoor exposure of the general population;
(c) $\rho = 3\ g\ cm^{-3}$ for the particle density;
(d) $\chi = 1.5$ for the particle shape factor.

The reference values for breathing and physiological parameters are also provided for Caucasian males and females, 15 years old males and females, and 10-, 5- and 1-year-old children, as well as 3 months old infants.

3.5. Clearance model

The materials deposited in the human respiratory tract are cleared with different mechanisms. These processes transfer the radioactivity from the lung into other organs and tissues in the body, so consideration of the clearance is also important for dose determination for other organs of the body.

Extensive studies of clearance of materials deposited in the lung have been performed in the past. The literature survey about clearance is given in Annex E of the ICRP66 report. However, many uncertainties involved in clearance still remain. The materials deposited in the human lung are cleared through three main routes:

(i) into blood by absorption;
(ii) to the gastrointestinal tract;
(iii) to regional lymph nodes via lymphatic tubes.

Route (i) is regarded as "absorption", while routes (ii) and (iii) are regarded as translocation. These processes are independent and they are in competition in each anatomical region of the respiratory tract. In addition, the materials deposited in the ET region can be removed by extrinsic means (e.g., nose blowing). The clearance rate λ_i defined as the part of materials $dR_i(t)/R_i(t)$ cleared per unit time:

$$\lambda_i(t) = \frac{dR_i(t)/dt}{R_i(t)} \tag{16}$$

The total clearance rate is the sum of the rates due to individual processes:

$$\lambda_i(t) = g_i(t) + l_i(t) + s_i(t) \tag{17}$$

where $g_i(t)$ is the rate of particle transport to the gastrointestinal tract, $l_i(t)$ is that to the lymph nodes and $s_i(t)$ is the rate of particle absorption into the blood.

Clearance of an anatomical region is represented by the three routes as shown in Fig. 4. Fig. 4 presents the clearance model for a completely insoluble material. For a soluble or partially soluble material, transport into blood applies for all compartments except ET_1. The particle transport rate shown in Fig. 4 as the number attached to the arrows are given in day^{-1}. These parameters are influenced by different factors such as smoking, age and disease.

The majority of the particles are cleared by mucous transport over the surface (including ET_2) towards the pharynx, where they are swallowed. However, a small part of the particles in the ET, BB and bb regions are retained in the airway walls and these are represented by the sequestration compartments (numbers 6, 9 and 12).

3.5.1. Extrathoracic airways

Most of the materials deposited in ET_1 are cleared by nose blowing, wiping, etc., with the clearing rate of $1\ d^{-1}$ (half time $t_{1/2} = 17$ h). The surfaces of the ET_2 region are covered by a fluid that is cleared to the pharynx with a time scale in the order of minutes. The reference value for the clearance rate from ET_2 to the GI tract is $100\ d^{-1}$ ($t_{1/2} \approx 10$ min). A small part of the particles (0.0005) deposited in ET_2 is sequestered. These are cleared to the lymph nodes LN_{ET} with the rate of $0.001\ d^{-1}$ ($t_{1/2} = 700$ d).

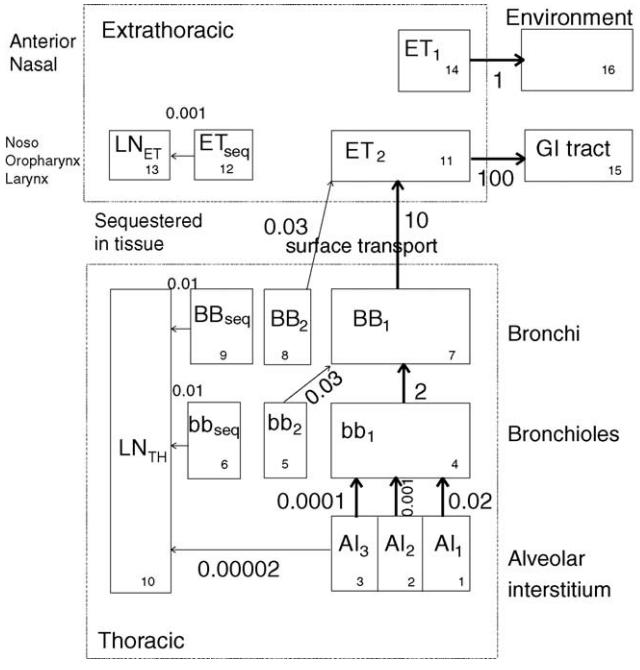

Fig. 4. Compartment model which shows particle transport from each region. The transport rate constants are given in d^{-1} (adopted from Ref. [7]).

3.5.2. Thoracic regions

The materials deposited in the BB and bb regions are subjects of fast clearing. These materials are dissolved in the mucous layer lining the surface of the airway tubes. The mucous moves upward and carries the dissolved particles towards the pharynx. In this way, the deposited particles are translocated from the site of deposition. The velocity of the mucous is a critical parameter. ICRP66 recommended the values 10 and 2 d^{-1} for the mucous clearance rate from the BB region to the pharynx, and from the bb region to the BB region, respectively.

Part of the materials deposited in the BB and bb regions is cleared slowly. For this reason, slowly cleared compartments (numbers 5 and 8) are introduced. The particles are transported from these compartments through the airway surface. The clearance rate from this compartment is taken as 0.03 d^{-1} ($t_{1/2}$ = 23 d). Prolonged retention in the airway wall is described by the sequestration compartments BB_{seq} and bb_{seq}. ICRP66 assumes that a fraction of 0.007 of the deposited material is sequestered in the BB and bb regions. The sequestered activity is cleared to the lymph nodes with the rate of 0.01 d^{-1}.

The alveolar interstitial region is cleared slower than the BB or bb regions. Retention of insoluble particles in the alveolar region can be very long, even longer than a year. Experimental data suggested that the AI anatomical region should be considered as three sub-compartment regions, namely, AI_1, AI_2 and AI_3, as shown in Fig. 4. The clearance rates from these sub-compartments towards the bb region are 0.02, 0.001 and 0.0001 d^{-1}.

3.5.3. Absorption into blood

The commission also assumes that absorption into blood happened with the same rate $s(t)$ in all considered regions except ET_1 where there is no absorption. This process consists of two steps. The first one is dissolution of the material into a form that blood can uptake. The second one is the absorption of dissolute materials into blood. Absorption into blood is very dependent on the chemical form of the deposited material. The absorption rates for different materials have a very wide range from 100 d^{-1} (for very soluble materials) up to 0.0001 d^{-1}.

In ICRP30 [6], the DWY classification scheme for the total particle clearance was presented. In ICRP66, the new classification F (fast), M (moderate), and S (slow) was adopted, and referred only to absorption into blood. Type F denotes the particles which are absorbed fast from BB, bb and AI, and 50% of materials deposited in ET_2. For type M, 70% of the materials deposited in AI reach the blood, while 10% of those deposited in the BB and bb regions and 5% of those in ET_2 also reach the blood. Type S denotes the materials that are little absorbed from ET, BB, bb into blood and 10% of those deposited in the AI region reach the blood.

3.6. Weighting the doses

The following weighting scheme was recommended (see also Eqs. (4) and (5)). The dose D_{BB} in the BB region is obtained as the average of the dose $D_{BB,bas}$ for basal cells and $D_{BB,sec}$ for secretory cells, i.e.,

$$D_{BB} = 0.5(D_{BB,bas} + D_{BB,sec}) \quad (18)$$

The dose D_{bb} in the bb region is equal to the dose for the secretory cells in this region, i.e.,

$$D_{bb} = D_{bb,sec} \quad (19)$$

The mean dose D for the respiratory track is then found as

$$D = 0.333(D_{BB} + D_{bb} + D_{AI}) \quad (20)$$

where D_{AI} is the absorbed dose in the AI region.

There are two inherent assumptions in this weighting scheme. The first one is the equal sensitivity of basal and secretory cells in the BB region, which might not be true. From the analysis of doses received by secretory and basal cells, and number of alpha hits in these cells, Nikezic and Yu [13] concluded that basal cells are more sensitive than secretory ones. The second one is the equal sharing of radiation detriment among the three regions (BB, bb and AI), where the same weighting factor $A_{BB} = A_{bb} = A_{AI} = 0.333$ was applied to each of them. The remaining 0.001 was used for lymphatic tissues. This assumption is more critical because it is known that the majority of lung cancers have origins in the upper part of the T-B tree.

4. Comparisons between different models

In the previous sections, some main characteristics of ICRP66 model were reviewed. However, in the literature, there were other dosimetric lung models. Here we will not elaborate all models that have appeared in the literature. Instead, some comparisons between the models will be given here.

4.1. Comparison between different morphometric models

From the morphometric point of view, two models appeared before the ICRP66 report, namely, the Yeh–Schum model [11] and the Weibel model [10]. The Yeh–Schum model considered the asymmetric structure of the human lungs with two lobes on the left hand side and three lobes on the right hand side. The non-dichotomous structure and asymmetric branching in the generations were also taken into account. The dimensions were given for all generations between 0 and 16 of the T-B tree. However, other parts of the respiratory tract, viz., ET and AI, were not described in full details. In contrary to the Yeh–Schum model, the Weibel model was completely symmetrical.

The Yeh–Schum model had a much larger volume than other models. For the purpose of comparison, therefore, its dimensions had to be scaled down. The procedures follow those described by James [14], i.e., all dimensions were multiplied with the factor 0.908. Since the lengths and diameters of airway tubes for the 15th and 16th generations were not given for all lobes in the original Yeh–Schum model, these were determined as follows. The unknown diameter for generation i was determined by the formula $d_i = d_i 2^{-1/3}$ [7] if the diameter was known for generation $(i-1)$, and the airway length was found based on the constant length-to-diameter ratio. The surface areas of the T-B tree for

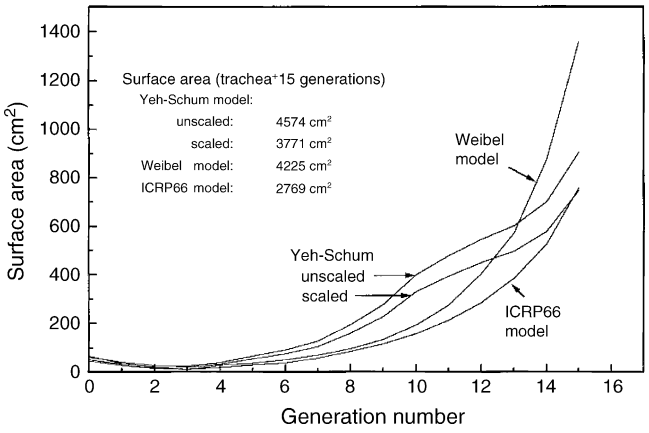

Fig. 5. The variation of surface area with the generation number for Weibel, ICRP66 and Yeh–Schum (scaled and unscaled) models. The total surface areas are also given.

different models are shown in Fig. 5. Computer programs were written to compare these different models. Only the morphometry was varied while keeping all other aspects the same. The results were given by Nikezic et al. [15], and are shown here in Figs. 6–9. The use of the Weibel and ICRP66 lung morphometry models led to larger DCCs than the Yeh–Schum model.

4.2. Comparison of different deposition models

As regards radon progeny deposition in the human lungs, there have been different approaches adopted by different groups of investigators. These approaches include the employment of the Gormley–Kennedy (G–K) expression [16], with or without corrections given by Martin and Jacobi [17]; Ingham (I) expression [18]; empirical expressions of Cohen and Asgharian [19] (C–A) and equations of Yu and Cohen [20] (Yu–C). The following are examples of groups of investigators who have adopted different approaches: G–K has been used by Porstendorfer [21] and Leung et al. [22]; I by Zock et al. [23], Nikezic et al. [15],

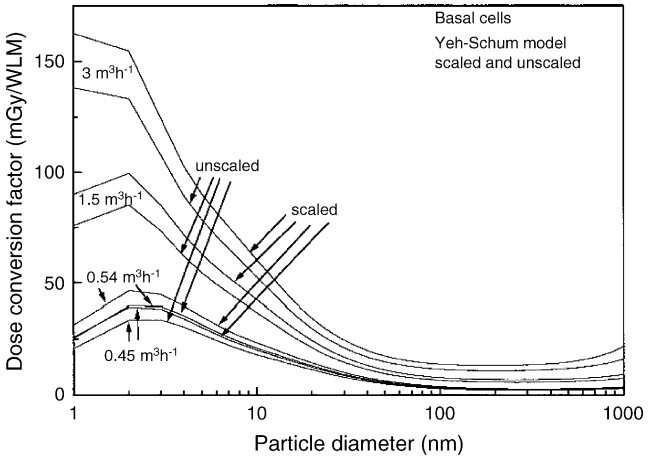

Fig. 6. The dose conversion factors for basal cells obtained using the Yeh–Schum models (scaled and unscaled) as a function of the particle diameter. The results were for 0.45, 0.54, 1.5 and 3 $m^3\ h^{-1}$ of inhaled air corresponding to various levels of physical activities, viz., sleep, rest, light and heavy exercise, respectively.

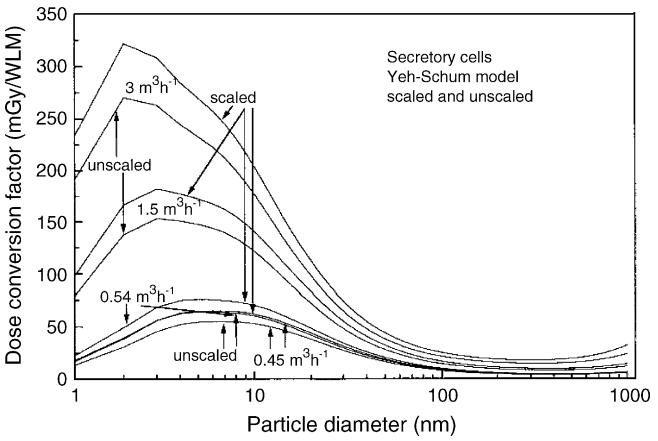

Fig. 7. The dose conversion factors for secretory cells obtained using the Yeh–Schum models (scaled and unscaled) as a function of the particle diameter. The results were for 0.45, 0.54, 1.5 and 3 $m^3\ h^{-1}$ of inhaled air corresponding to various levels of physical activities, viz., sleep, rest, light and heavy exercise, respectively.

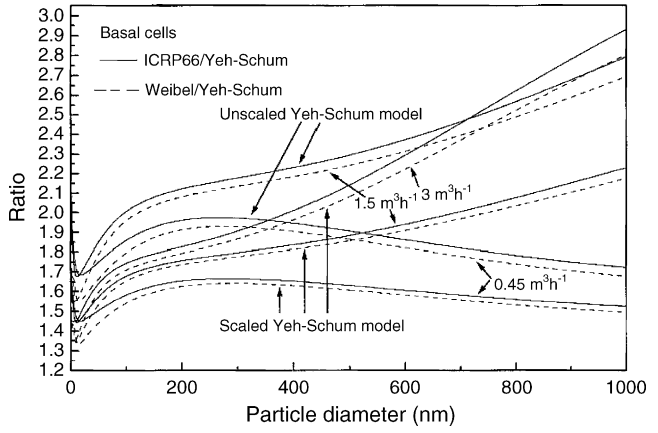

Fig. 8. Ratio between the dose conversion factors for basal cells given by the ICRP66 and Yeh–Schum models (solid lines) and ratio between the dose conversion factors given by the Weibel and Yeh–Schum models (dashed lines) for 0.45, 1.5 and 3 $m^3\ h^{-1}$ of inhaled air. The curve for unscaled Yeh–Schum model for 3 $m^3\ h^{-1}$ is not shown to avoid too many curves.

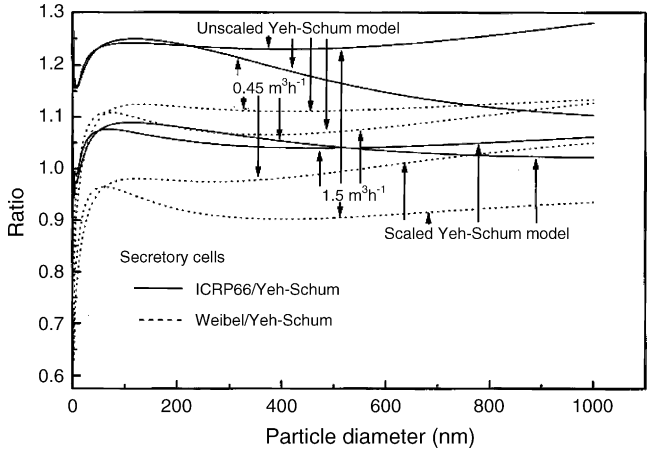

Fig. 9. Ratio between the dose conversion factors for secretory cells given by the ICRP66 and Yeh–Schum models and ratio between the dose conversion factors given by the Weibel and Yeh–Schum models for 0.45 $m^3\ h^{-1}$ of inhaled air.

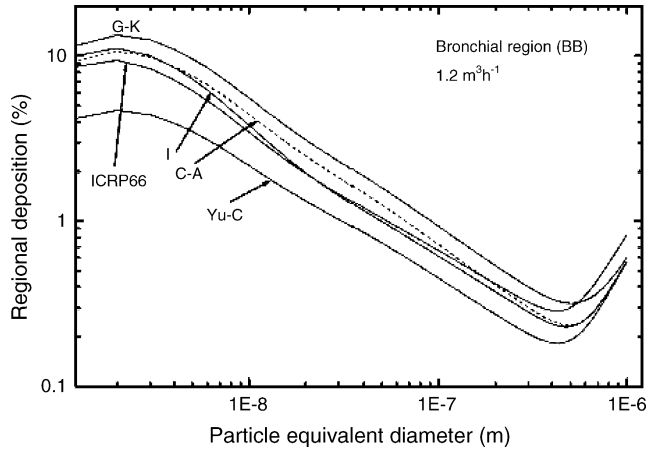

Fig. 10. Regional deposition in the BB region for a breathing rate of 1.2 $m^3\ h^{-1}$.

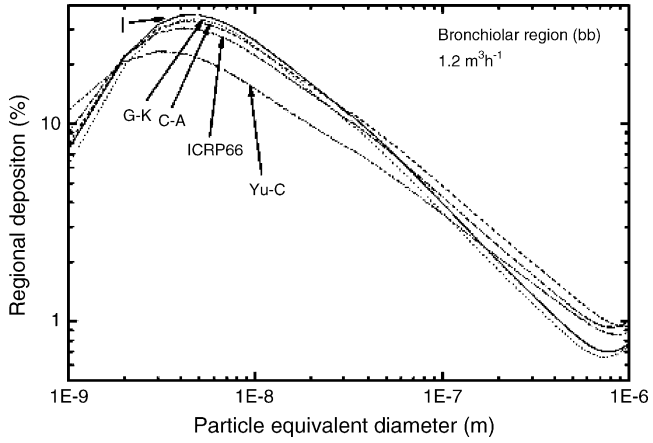

Fig. 11. Regional deposition in the bb region for a breathing rate of 1.2 $m^3\ h^{-1}$.

Hofmann et al. [24], ICRP [7]; C–A by Harley et al. [25]; Yu–C also by ICRP [7]. Nikezic et al. [26] compared these formulae and investigated their influences on the DCC. Only the results for comparison are presented here (without detailed description of the formulae in Table 8). Depositions in the BB and bb regions calculated with different formulae are given in Figs. 10 and 11, respectively. The calculations were performed for the breathing rate of 1.2 $m^3\ h^{-1}$.

Inconsistencies among the results obtained from different formulae have been identified through all particle ranges. The discrepancies can be caused by different assumptions and methods used in the derivations of the formulae. The largest difference among the results from various deposition formulae is found in the unattached particle range. However, unattached particles contribute significantly (although their contribution is smaller than attached progeny) to the dose so the unreliable deposition efficiencies in this region can introduce uncertainties in the final value for DCCs.

The results of DCC calculations are given in Table 8 for four different breathing rates, which represent different levels of physical activities of an adult Caucasian male—sleep: 0.45 $m^3\ h^{-1}$; light exercises: 1.5 $m^3\ h^{-1}$; heavy exercises: 3 $m^3\ h^{-1}$ [27]; and for the average weighted physical activity: 0.78 $m^3\ h^{-1}$ [28].

The difference between DCCs obtained using various deposition formulae can be as much as 30%. This difference is not unimportant but it is still smaller than the uncertainty introduced by other factors involved in DCC calculations [28,29].

5. Dependence of DCC on various parameters in the lung model

The human lung model consists of many parameters. These parameters include (a) aerosol parameters, (b) subject related parameters, (c) target and cell related parameters, and (d) parameters that define the absorption of radon from lung to blood. All these parameters, in one way or the other, affect the DCC. Some parameters are very important in the DCC calculations while others are less important. Marsh and Birchall [28] conducted sensitivity analyses to identify the influence of parameters on DCCs. They varied one parameter in a reasonable range at one time, while keeping all others at their best estimates. To characterize the influence of the parameters, a reliability factor r was introduced which was defined as $r = \sqrt{\mathrm{DCC_{max}/DCC_{min}}}$, where $\mathrm{DCC_{max}}$ and $\mathrm{DCC_{min}}$ were obtained for the maximal and minimal values, respectively, of a given parameter.

The most important aerosol parameter was the unattached fraction which had a reliability factor of 1.71. The breathing rate, with a reliability factor of 1.59, was the most important subject related parameters. The most important target-cell parameters were the depth of the sensitive cells and the thickness of tissues, which had reliability factors of 1.64. The lung-tissue weighting factor A_{BB}, A_{bb} and A_{AI}, which were assigned as 0.333, were also very important. For example, if these factors were varied from (0.25, 0.25, 0.5) to (0.8, 0.15, 0.05), the DCC was changed from 21 to 11 mSv/WLM. All other parameters were of less importance.

Table 8
Dose conversion factors calculated by using different deposition formulae (adopted from Ref. [26])

Breathing rate ($m^3\ h^{-1}$)	Breathing frequency (min^{-1})	Dose conversion factors (mSv/WLM)				
		Ingham	Cohen–Asgharian	Gormley–Kennedy	Yu–Cohen	ICRP66 deposition
0.45	15	9.37	9.73	8.59	7.31	7.68
0.78	20	13.61	14.56	12.73	10.62	11.77
1.5	20	21.27	23.02	20.39	15.93	18.25
3.0	26	36.82	41.0	36.1	28.51	34.29

The same program (except for ICRP66) has been used for all calculations.

All in all, the DCC ranged between 8 and 33 mSv/WLM, with a central value of about 15 mSv/WLM which is considered as the dosimetric result. However, there are criticisms about this kind of sensitivity analyses of the parameters, since in reality not only one parameter is varying while all others are at their best estimated values. In order to address these critics, Marsh et al. [30] conducted another uncertainty analysis by varying all the parameters according to their own distributions. They also emphasized the lack of experimental data for some parameters. The results gave a mean DCC value in the vicinity of 15 mSv/WLM.

6. Epilogue

The dosimetric calculations gave a central value for DCC of 15 mSv/WLM. However, there is another estimation for DCC derived from epidemiological studies of miners. This epidemiological result is $DCC_{ep} = 5$ mSv/WLM. ICRP66 stated that dosimetric models should only be used for comparison of doses in the human lungs resulted from different exposure conditions. For estimation of the health risk, the ICRP66 recommended the use of the epidemiological result.

A proposal to reconcile this difference was lowering the radiation weighting factor for alpha particles from 20 to 10 or even less [9]. This will bring DCC to the value of about 8 mSv/WLM, which is not too different in comparison to epidemiological result. Other attempts include the use of microdosimetric approach [13,31–33].

References

[1] International Commission on Radiological Protection, Limits for inhalation of radon daughters by workers: A Report of the International Commission on Radiological Protection: ICRP Publication 32, Pergamon Press, Oxford, 1981.
[2] R.L. Fleischer, in: S.A. Durrani, R. Ilic (Eds.), Radon Measurements by Etched Track Detectors, World Scientific, Singapore, 1997, p. 3.
[3] International Commission on Radiological Protection, Recommendations of ICRP Publication 60, Pergamon Press, Oxford, 1990.
[4] International Commission on Radiological Protection, Recommendation of the International Commission on Radiological Protection, Report of Committee II on Permissible Dose for Internal Radiation (1959). ICRP Publication 2, Pergamon Press, Oxford, 1960.
[5] Task Group on Lung Dynamics (TLGD), Health Phys. 12 (1966) 173.
[6] International Commission on Radiological Protection, Limits for Intakes of Radionuclides by Workers, ICRP Publication 30, Pergamon Press, Oxford, 1979.
[7] International Commission on Radiological Protection, Human respiratory tract model for radiological protection: A report of a Task Group of the International Commission on Radiological Protection, ICRP Publication 66, Pergamon Press, Oxford, 1994.
[8] A. Birchall, M.R. Bailey, A.C. James, Radiat. Prot. Dosim. 38 (1991) 167.
[9] J.W. Marsh, A. Birchall, Radiat. Prot. Dosim. 87 (2000) 167.
[10] E.R. Weibel, Morphometry of the Human Lung, Springer, Berlin, 1963.
[11] H.C. Yeh, G.M. Schum, Bull. Math. Biol. 42 (1980) 461.
[12] R.F. Phalen, M.J. Oldham, C.B. Beaucage, T.T. Crocker, J.D. Mortensen, Anat. Rec. 212 (1985) 368.
[13] D. Nikezic, K.N. Yu, Int. J. Radiat. Biol. 77 (2001) 559.
[14] A.C. James, Dosimetry aspects of exposure to radon and thoron daughter product, Report by a Group of Experts of the OECD Nuclear Energy Agency, 1983.
[15] D. Nikezic, K.N. Yu, T.T.K. Cheung, A.K.M.M. Haque, D. Vucic, J. Environ. Radioact. 47 (2000) 263.
[16] P.G. Gormley, M. Kennedy, Proc. Irish Acad. 52A (1949) 163.
[17] D. Martin, W. Jacobi, Health Phys. 23 (1972) 23.
[18] D.B. Ingham, J. Aerosol Sci. 6 (1975) 125.
[19] B.S. Cohen, B. Asgharian, J. Aerosol Sci. 21 (1990) 789.
[20] C.P. Yu, B.S. Cohen, in: J. Dodgson, R.L. McCallum (Eds.), Proceedings of the VII International Symposium on Inhaled Particles, 1994.
[21] J. Porstendorfer, Environ. Int. 22 (Suppl. 1) (1996) S563.
[22] J.K.C. Leung, M.Y.W. Tso, C.W. Ho, L.C. Hung, Radiat. Prot. Dosim. 71 (1997) 289.
[23] C. Zock, J. Porstendorfer, A. Reineking, Radiat. Prot. Dosim. 63 (1996) 197.
[24] W. Hofmann, G. Mainelis, A. Mohammed, I. Balashazy, J. Vaupotic, I. Kobal, Environ. Int. 22 (Suppl. 1) (1996) S965.
[25] N.H. Harley, B.S. Cohen, E.S. Robins, Environ. Int. 22 (Suppl. 1) (1996) S959.
[26] D. Nikezic, A.K.M.M. Haque, K.N. Yu, J. Environ. Radioact. 61 (2002) 305.
[27] National Research Council, Comparative Dosimetry of Radon in Mines and Homes, Panel on Dosimetric Assumption Affecting the Application of Radon Risk Estimates, National Academy Press, Washington, DC, 1991.
[28] J.W. Marsh, A. Birchall, Radiat. Prot. Dosim. 87 (2000) 167.
[29] A. Birchall, A.C. James, Radiat. Prot. Dosim. 53 (1994) 133.
[30] J.W. Marsh, A. Birchall, G. Butterweck, M.-D. Dorrian, C. Huet, X. Ortega, A. Reineking, G. Tymen, Ch. Schuler, A. Vargas, G. Vessu, J. Wendt, Radiat. Prot. Dosim. 102 (2002) 229.
[31] D. Nikezic, K.N. Yu, Radiat. Environ. Biophys. 40 (2001) 207.
[32] D. Nikezic, K.N. Yu, Radiat. Res. 157 (2002) 92.
[33] D. Nikezic, K.N. Yu, Int. J. Radiat. Biol. 78 (2002) 605.